Title

Incidence of metal-based nanoparticles in the conventional wastewater treatment process

Authors

Cervantes-Avilés, Pabel
Keller, Arturo A

Publication Date

2021-02-01

DOI

10.1016/j.watres.2020.116603

Peer reviewed

Water Research 189 (2021) 116603

Contents lists available at ScienceDirect

Water Research

journal homepage: www.elsevier.com/locate/watres

Incidence of metal-based nanoparticles in the conventional wastewater treatment process

Pabel Cervantes-Avilés [a,c], Arturo A. Keller [b,c,*]

[a] Tecnologico de Monterrey, Escuela de Ingeniería y Ciencias, Reserva Territorial Atlixcáyotl, Puebla, Pue, CP 72453, Mexico
[b] Bren School of Environmental Science and Management, University of California at Santa Barbara, CA, 93106, USA
[c] University of California, Center for Environmental Implications of Nanotechnology, Santa Barbara, CA, 93106, USA

ARTICLE INFO

Article history:
Received 25 June 2020
Revised 28 October 2020
Accepted 3 November 2020
Available online 6 November 2020

Keywords:
Wastewater
Sludge
Multi-element determination
Rate of NPs
NPs size distribution
Spicp-MS

ABSTRACT

Metal-based nanoparticles (NPs) can be found in wastewater streams, which are significant pathways for the release of NPs to the environment. Determination of the NPs concentration in wastewater streams is important for performing appropriate ecotoxicological evaluations. The aim of this work was to determine the incidence of NPs from 13 different elements throughout the wastewater treatment process by using single particle inductively coupled plasma mass spectrometry (spICP-MS). The incidence was determined in samples of the influent, post-primary treatment and effluent of the activated sludge process, as well as in the reclaimed water of a full-scale wastewater treatment plant (WWTP). In addition, concentration of NPs was determined in the waste activated sludge and in the anaerobic digester. The concentration of metal-based NPs in the influent wastewater were between 1,600 and 10,700 ng/L for elements such as Ti, Fe, Ce, Mg, Zn and Cu, while that for Ni, Al, Ag, Au, Co and Cd was below 100 ng/L. Concentrations in reclaimed water ranged between 0.6 and 721 ng/L, ranked as Mg > Ti > Fe > Cu > Ni > Ce > Zn > Mn > Al > Co > Ag > Cd > Au. Results indicated that the activated sludge process and reclaimed water system removed 84–99% of natural and engineered metal-based NPs from influent to reclaimed water, except for Mg, Ni and Cd where the removal ranged from 70 to 78%. The highest concentrations of NPs were found in the waste activated sludge and anaerobic sludge, ranging from 0.5 to 39,900 ng/L. The size distribution of NPs differed in different wastewater streams within the WWTP, resulting in smaller particles in the effluent (20–180 nm) than in the influent (23–233 nm) for most elements. Conversely, NPs were notably larger in the waste activated sludge samples than in the anaerobic sludge or wastewater, since conditions in the secondary treatment lead to precipitation of several metal-based NPs. The incidence of metal-based NPs from 13 elements in wastewater decreased significatively after the conventional wastewater treatment train. However, anaerobic digesters store high NPs concentrations. Hence, the disposal of sludge needs to take this into account to evaluate the risk of the release of NPs to the environment.

1. Introduction

Confirming the presence of engineered or natural nanoparticles (NPs), and monitoring their concentrations in the environment are essential to understand their potential implications in environmental matrices. Due to the wide range of applications of NPs in daily life products (e.g. textiles, cleaning agents, personal care products), wastewater streams receive significant loads of NPs, with diverse composition and a wide range of concentrations according to predictions (Lazareva and Keller, 2014; Sun et al., 2016). Although wastewater treatment plants (WWTP) can potentially remove over 90% of the influent load of several NPs such as Ag, SiO_2, TiO_2 or CeO_2 (Cervantes-Avilés et al., 2018; Westerhoff et al., 2018), it is possible that the residual concentrations of some NPs and transformation products in the effluent can affect some organisms in the aquatic ecosystems such as algae, crustaceans and fish cells on the reproduction and growth stages (Georgantzopoulou et al., 2018). Since the fate of biosolids from WWTP are landfills, incineration plants and agricultural soils (Keller and Lazareva, 2013; Sun et al., 2016; Wang et al., 2016), determining the NPs concentration in the sludges of secondary treatment is also relevant, and quite challenging due to high ratio of solid to liquid phases in the matrix, and the physical, chemical and biological interactions between NPs and sludge of the WWTP. To determine their risk, accurate quantification of NPs in wastewater and sludges is needed.

Several methods used for nanometrology and characterization of NPs after synthesis have been applied for measuring

* Corresponding author.
E-mail address: keller@bren.ucsb.edu (A.A. Keller).

https://doi.org/10.1016/j.watres.2020.116603
0043-1354/

their concentrations (mass, surface area, number) in environmental matrices (Palchoudhury et al., 2015). For determining mass concentration of NPs in environmental complex media, graphite furnace atomic absorption spectroscopy (GF AAS) (Li et al., 2013), inductively coupled plasma mass spectrometry (ICP-MS) (Choi et al., 2017; Kaegi et al., 2011), ICP optical emission spectroscopy (ICP-OES) (Contado and Pagnoni, 2010; Ortelli et al., 2017), surface-enhanced Raman spectroscopy (SERS) (Guo et al., 2016), field flow fractionation ultraviolet-visible spectroscopy (FFF-UV) (Bednar et al., 2013) have been previously used. However, issues regarding detection limits, reproducibility, transformation of NPs and versatility in handling diverse environmental matrices, have affected the analysis of real environmental matrices (Lead et al., 2018; Lowry et al., 2012b), limiting the ability to accurately detect and quantify NPs in these samples.

ICP-MS based techniques have been shown to be sensitive enough to detect and quantify NPs at low concentrations in the environment (Fréchette-Viens et al., 2019). Single particle ICP-MS (spICP-MS) has emerged as a reliable technique to size and quantify NPs extracted from soil (Schwertfeger et al., 2017), and in various aqueous media (Bi et al., 2015; Degueldre and Favarger, 2003; Laborda et al., 2019, 2013; Montaño et al., 2019), including the concentration of specific NPs in wastewater (Bevers et al., 2020; Cervantes-Avilés et al., 2019a; Hadioui et al., 2015; Mitrano et al., 2012; Proulx et al., 2016). In this technique, the passage of a single NP produces a flash of ions in the ICP that generate a large transient signal. Acquisition and quantification of each of these events in Time-Resolved Acquisition (TRA) mode allows the determination of the number of particles in a given sample volume (Laborda et al., 2014; Montaño et al., 2014). The signal intensity of each measured NP is then converted to a mass, using information from a reference material (e.g. Au or Ag nanoparticles), the nebulization efficiency (or transport efficiency), assumptions about the composition of the NP, and the determination of the baseline for each element or analyte.

Single element analysis of NPs in wastewater and surface water samples via spICP-MS has included: Ag (Cervantes-Avilés et al., 2019a; Heithmar and Pergantis, 2010; Mitrano et al., 2012; Proulx et al., 2016; Tuoriniemi et al., 2017), Au (Laborda et al., 2016), Ti (Bitragunta et al., 2017; Gondikas et al., 2018; Heithmar and Pergantis, 2010; Tuoriniemi et al., 2012), Cu (Navratilova et al., 2015), Ce (Bi et al., 2015; Heithmar and Pergantis, 2010; Tuoriniemi et al., 2012), Fe (Heithmar and Pergantis, 2010), Al (Bi et al., 2015) and Zn (Bevers et al., 2020; Hadioui et al., 2015). Besides, previous studies have screened up to 40 elements in DI water via spICP-MS (Lee et al., 2014; Tuoriniemi et al., 2012), one element per run was detected and quantified, which entailed a long measurement time to perform the analysis for a wide range of elemental compositions of the NPs. Until now, measurements of several isotopes during a run for NP detection have been achieved modifying a time-of-flight instrument, with some trade-offs such as data analysis, lower sensitivity for some elements and drift (Borovinskaya et al., 2013). Hence, the ability to detect several elements and isotopes in a single run using spICP-MS can significantly reduce the overall run time and cost.

Distinguishing NP signals from the ionic background (dissolved analyte) is another issue when spICP-MS is applied (Cornelis and Hassellöv, 2014; Hadioui et al., 2014), limiting the detection of small NPs. This is particularly challenging for samples with polydisperse NP size distributions and for complex matrices such as biosolids that contains high ionic background. To overcome these difficulties and provide extra information about NPs, discrimination and fractionation techniques, as well as separation systems coupled to ICP-MS have been investigated, such as field-flow fractionation (FFF) (M. D. Montaño et al., 2014), hydrodynamic chromatography (HDC) (Pergantis et al., 2012; Proulx et al., 2016), high performance liquid chromatography (HPLC)(Ta et al., 2014), capillary electrophoresis (CE) (Mozhayeva and Engelhard, 2017; Qu et al., 2014), electrospray-differential mobility analysis (ES-DMA) (Tan et al., 2016) and ion exchange resins (IER) (Azimzada et al., 2017; Hadioui et al., 2014). IER is relatively easy to operate and has been successfully applied to remove the dissolved form of several NPs (Azimzada et al., 2017; Cervantes-Avilés et al., 2019b; Fréchette-Viens et al., 2019), improving the particle size detection limits during spICP-MS (Hadioui et al., 2014). Although the IER-spICP-MS has been applied to detect and quantify NPs of one element at a time (Hadioui et al., 2014), its application to detect multiple elements in wastewater has not been studied. Therefore, the application and comparison of IER-spICP-MS and spICP-MS for NP detection and sizing in wastewater can contribute to understanding of the influence of IER when analyzing multiple elements, determining detection thresholds, and even to detect NP based on elements without evidence of their presence in wastewater such as Ni, Cd, Co, Mn and Mg. This could be possible due to the IER is able to adsorb multiple cations in a wide pH range (4–10), which covers the typical pH range of wastewater (6–8).

The overall aim of this work was to determine the incidence of NPs from 13 elements and their size distribution in samples from different locations within a WWTP, such as influent, post-primary, effluent, reclaimed water, waste activated sludge and the anaerobic digester. The specific objectives were to: (1) evaluate the use of IER before spICP-MS to improve the quantification and sizing of NPs based on 13 different elements by comparing its application with conventional spICP-MS; (2) determine the incidence of NPs in the influent, post-primary, effluent and reclaimed water of a full scale WWTP using the IER-spICP-MS approach; and (3) determine the size distributions of the analyzed NPs in collected samples at different locations of the WWTP. The goal is to provide valuable information on the concentrations and size of these different NPs in wastewater effluent and sludge for realistic risk assessment.

2. Materials and methods

2.1. Materials

Ultrapure water (DI) with a resistivity of 18.2 MΩ-cm was obtained from a NANOpure water purification system (Thermo Scientific) and used for preparation of NPs suspensions and ionic solutions. A multi-element standard solution containing 10 mg/L of aluminum (Al), cadmium (Cd), cerium (Ce), cobalt (Co), copper (Cu), iron (Fe), magnesium (Mg), manganese (Mn), nickel (Ni), titanium (Ti) and zinc (Zn) in 5% HNO_3, was purchased from Agilent Technology (Santa Clara, CA, USA). Single element standard solutions of Ag (10 mg/L) and Au (100 mg/L) in 2% HNO_3 and 2% HCl, respectively, were also acquired from Agilent Technologies. HCl (34–37%) and HNO_3 (67–70%) of ultra-high purity for quantitative trace metal analysis at the parts-per-trillion (ng/L) level (BDH Aristar® Ultra grade) were used to dilute the standard solutions used for calibration. Metal-free polypropylene tubes were used for preparation of suspensions and respective dilutions. Commercial suspensions of Au NPs and Ag NPs, both with a nominal diameter of 60 nm, were purchased from nanoComposix (San Diego, CA, USA) as dispersed NPs in 2 mM sodium citrate. Chelex-100 resin with 50–100 mesh and a capacity of 0.7 meq/mL was acquired from Sigma-Aldrich and packed in polypropylene tubes with 3.0 mm of internal diameter and 14 cm of effective length. Glass wool (Sigma-Aldrich) was placed at the beginning and end of the columns to contain the resin. NaOH (99.9%, trace metal basis, Sigma-Aldrich) and HCl (34–37%, ultra-high purity), both at 1 M, were used to regenerate the resin before each sample processing. Polypropylene syringes were used to inject the samples in the IER column prior spICP-MS analysis.

Table 1
Optimized instrumental setting for multi-element spICP-MS (Agilent 7900).

Parameter	Value
Reference material	100 ng/L, Au NPs 60 nm
RF Power	1550 W
Carrier gas	0.67 L/min
Spray chamber temperature	2 °C
Sample flow rate	0.346 mL/min
Sample depth	8.0 mm
Integration time	100 µs
Acquisition time per element	20 s
Settling time per element	5 s
Monitored isotopes	^{107}Ag, ^{27}Al, ^{192}Au, ^{111}Cd, ^{140}Ce, ^{59}Co, ^{63}Cu, ^{56}Fe, ^{24}Mg, ^{55}Mn, ^{60}Ni, ^{47}Ti, ^{66}Zn

2.2. Sampling and characterization of wastewater and sludge

Wastewater and sludge samples were collected from a municipal WWTP in southern California. Wastewater samples corresponded to the influent, post-primary treatment, effluent, and reclaimed water (Figure S1). Sludge samples were collected from the pipe port of the recirculation of activated sludge (RAS) and from the anaerobic digester (AD). Sampling points are indicated in the diagram presented in the Supporting Information (Figure S1). Before the sampling day, containers of 1 L made of low-density polyethylene with polypropylene caps were submerged in HNO_3 (10%) overnight. The day of sampling containers were rinsed three times with DI water. On site, the containers were rinsed three times with the respective water to be sampled before they were filled. Samples (1 L) were collected per triplicate in each sampling point and were stored at 4 °C until their characterization and spICP-MS analysis the next day.

Wastewater and sludge samples were analyzed in triplicate to determine the content of the total, volatile and fixed suspended solids (TSS, VSS and FSS) following the gravimetric method 2540 (APHA, 2005). Chemical oxygen demand (COD), total nitrogen (TN), ammonia (NH_4^+), nitrate (NO_3^-), nitrite (NO_2^-), orthophosphate (PO_4^{3-}), sulfide (S^{2-}) and turbidity were measured following commercial tests (Hach). Dissolved organic carbon in filtered samples (0.45 μm) was determined according to method 5310B (APHA, 2005).

2.3. spICP-MS settings and calibration

The spICP-MS analysis was performed with an Agilent 7900 ICP-MS. This instrument was used with platinum sampling and skimmer cones, a glass nebulizer (MicroMist), double pass cyclonic quartz spray chamber (Agilent), and quartz torch with an internal diameter of 1 mm. Samples were introduced directly into the ICP-MS with the standard peristaltic pump, through Tygon tubing with an internal diameter of 1.02 mm. When IER was used, samples were first passed through resin column in batch mode by using polypropylene syringes, then submitted to the spICP-MS. Data of the 13 elements of interest in a sample were collected sequentially during 325 s: 20 s per element in time resolved analysis (TRA) mode, using an integration time (dwell time) of 100 μs per point as previously reported (Bevers et al., 2020; Montaño et al., 2014), with a settling time of 5 s in between elements. Data analyses were performed using the Rapid Multi-Element Nanoparticle Analysis mode of the Single Nanoparticle Application Module of Agilent ICP-MS MassHunter software (Version C.01.05 Build 588.3). The instrumental settings used for the spICP-MS analysis are summarized in Table 1.

Calibration of the spICP-MS for NPs quantification was done by tuning the particle size of a reference material (Au NP, mentioned above) and determining the elemental response factor for reference material and analyzed elements. The 60 nm Au NP reference standard was diluted to 100 ng/L with DI to determine the nebulization efficiency (η_n), also known as transport efficiency, to be used in the data conversion from raw signal to NP size. Nebulization efficiency was 5.3%, calculated based on the particle size method (Pace et al., 2011). Eq. (1) shows the parameters considered for calculating η_n, where, d_{std} is the NP diameter (nm) in reference material, ρ_{std} is the reference material density (g/cm^3), s is the response factor of analyzed elements (cps/(µg/L)), I_P is the peak intensity of reference material or individual pulse intensity (cps), t_d is the dwell time (s), f_d is the reference material mass fraction (1), V is the sample flow rate (cm^3/min) and the conversion factors 60 (s/min) and 10^{12} (10^{21} nm^3/cm^3 • 10^{-3} L/cm^3 • 10^{-6} g/ µg). To verify that data collection from the Au NP reference material was suitable for consecutive elemental analysis, 100 ng/L of the 60 nm Ag NPs was also spiked into the reference material suspension and collected for size determination.

$$\eta_n = \frac{\frac{4}{3}\pi \times \left(\frac{d_{std}}{2}\right)^3 \times \rho_{std} \times s \times 60}{I_P \times t_d \times f_d \times V \times 10^{12}} \quad (1)$$

The multi-element standard solution containing 10 mg/L of all analytes was diluted from 0 to 1 μg/L with 1% HNO_3, to be used to determine the elemental response factor. NP size was calculated from the mass of the particle (m_p), as in Eqs. (2) and 3 (Laborda et al., 2014; Lee et al., 2014), assuming that NP density (ρ_p) is different for each of the 13 elements, but constant for the same element, and that the NPs are spherical. Concentration of NP (C_m) was determined according to Eq. (4), where, T, is the acquisition time (min) per element (0.33). The particle densities and analyte mass fractions for the 13 types of NPs are listed in the supporting information (Table S2).

$$d = 3\sqrt{\frac{6 \times m_p}{\rho_p \times \pi}} \quad (2)$$

$$m_p = I_p \times \frac{1}{s} \times t_d \times V \times \eta_n \times 10^6 \times f_d \times \frac{1}{60} \quad (3)$$

$$C_m = \frac{\sum m_p}{10^3} \times \frac{1}{\eta_n} \times \frac{1}{V} \times \frac{1}{T} \quad (4)$$

Dilution of Au NP reference material, sample preparation and dilution were performed on the day of the analysis to minimize transformations and NP solubilization after processing. Based on the concentration of previous studies detecting NPs in real wastewater (Cervantes-Avilés et al., 2019a; Mitrano et al., 2012), the samples and reference materials were diluted with DI water to ensure NP concentrations were between 10 and 100 ng/L. Before dilution of the samples, and again prior to the spICP-MS analyses, all suspensions were placed in an ultrasonic bath for 10 min at 280 W and a frequency of 40 kHz to ensure that the samples were fully homogenized.

Table 2
Concentration of major components, pH and turbidity of wastewater and sludge samples collected in a conventional wastewater treatment plant.

Parameter	Influent	Post Primary	Effluent	Reclaimed water	Waste sludge	Anaerobic sludge
pH	7.3 ± 0.2	7.3 ± 0.2	7.4 ± 0.1	7.0 ± 0.1	7.0 ± 0.1	7.7 ± 0.2
Conductivity (mS/cm)	2.7 ± 0.1	2.7 ± 0.1	2.3 ± 0.1	2.3 ± 0.1	3.1 ± 0.1	6.1 ± 0.7
COD (mg/L)	664±11	317±7	68±3	37±2	4270±360	22,323±380
DOC (mg/L)	238±11	189±6	11.5 ± 0.3	2.1 ± 0.4	323±7.5	1850±11
TN (mg/L)	159±5	94±5	26±1	6.2 ± 0.9	146±3.4	696±28
NH_4^+–N (mg/L)	57±2	39.2 ± 3	2.9 ± 0.2	2.7 ± 0.4	14.4 ± 3.3	504.2 ± 7
NO_3–N (mg/L)	3.2 ± 0.2	2.2 ± 0.2	11.3 ± 0.2	4.8 ± 0.9	12.7 ± 0.2	6 ± 0.2
NO_2–N (mg/L)	0.2 ± 0.1	0.8 ± 0.1	1.4 ± 0.1	1.2 ± 0.2	N/A	N/A
PO_4–P (mg/L)	16.8 ± 0.1	12.8 ± 0.1	3.6 ± 0.1	1.9 ± 0.1	5.2 ± 0.3	38±1.7
S^{2-} (mg/L)	6.3 ± 0.4	5.3 ± 0.2	<0.05	<0.05	<0.05	19.5 ± 1.3
Turbidity (NTU)	112	92	6.3	0.2	N/A	N/A
Suspended solids (SS)						
TSS (mg/L)	354±42	108±13	19.2 ± 14	<1	6820±117	25,300±890
VSS (mg/L)	285±31	98±10	16.0 ± 14	<1	5363±98	18,950±600
FSS (mg/L)	69±5	10±4	5 ± 3	<1	1457±80	6350±560

2.4. Procedure for detecting NPs in wastewater and sludge samples

The samples of wastewater and sludge were brought from 4 °C to room temperature (20 °C) before analysis. Wastewater samples were vortexed, then sieved through a 0.5 mm mesh (Sieve No. 35) to avoid deposit build-up in the sampler and skimmer cones (Tuoriniemi et al., 2017). Sludge samples were processed to extract metal-containing NPs according to our previous study (Huang et al., 2020). Briefly, samples of waste sludge and anaerobic sludge were ultrasonicated 20 min at 280 W and a frequency of 40 kHz. Then, samples were centrifuged for 10 min at 4000 g to separate the suspended biomass. The supernatant of wastewater and anaerobic sludge were diluted 100 times with ultrapure water. In order to evaluate the influence of using an IER for ions removal prior spICP-MS analysis of multiple elements, wastewater and sludge samples were divided in three sets. The three sets of samples were ultrasonicated for 10 min at 280 W and a frequency of 40 kHz; It should be considered that sonication may influence dissolution and aggregation of NPs (Taurozzi et al., 2012). One set of samples was submitted immediately to the spICP-MS for consecutively elemental analysis, without passing through the IER column. In the second set of samples was evaluated the removal of NPs in the IER by spiking 100 ng/L of Ag in the collected samples, then passing 5 mL of sample through the IER column packed with Chelex-100, and finally analyzing them by spICP-MS. The third set of wastewater and sludge samples was also passed through the IER column packed with Chelex-100 prior to spICP-MS analysis for particle quantification. Before each sample run using the IER, the column was regenerated by sequentially washing it with 5 mL of 1 M HCl, 5 mL of DI water at pH 7, 5 mL of 1 M NaOH, and 5 mL of DI water at pH 7. The spICP-MS and IER-spICP-MS analyses were performed in triplicate, and the results of mass concentration and mean size were the average of the replicates.

3. Results and discussion

3.1. Wastewater treatment and sludge characteristics

The wastewater treatment in the studied system effectively removed soluble carbon, nitrogen, and phosphorous (Table 2). Several ligands and suspended solids related with particle stability (Hotze et al., 2010) were measured. A higher concentration of S^{2-} was observed in the influent, post-primary wastewater and anaerobic sludge liquor, compared to other locations. Hence, sulfidation of metal-based NPs, especially chalcophile elements (E.g. Cu, Zn, Cd, Ag) is expected at these points due to long hydraulic retention times, such as the secondary treatment (4–6 h) and the anaerobic digester (up to 10 d). Moreover, the formation of sulfuric coatings on the surface of NPs can suppress the release of ions from metal-based NPs made of chalcophile elements. The interaction of other relevant ligand, such as PO_4^{3-}, with metal-based NPs has been reported as a stabilizing agent or even forming a shell of amorphous crystal in some NPs (Rathnayake et al., 2014). These processes can occur in high content phosphate streams such as the influent (16.8 mg PO_4^{3-}/L) and anaerobic sludge liquor (38 mg PO_4^{3-}/L). Regarding the TSS content, the concentration found in the influent, waste and anaerobic sludge were 354 mg/L, 6820 mg /L and 25,300 mg/L respectively. The high concentration of TSS in such points suggest the hetero-aggregation of NPs with the biomass, precipitating in the activated sludge reactors or anaerobic digesters (Barton et al., 2015; Hotze et al., 2010; Wang et al., 2015). Moreover, higher conductivity in anaerobic sludge compared to waste sludge may also indicate a higher accumulation of metal-based NPs in the anaerobic digester (Table 2). Conversely, stabilization of particles has been observed in the presence of organic matter, as dissolved organic carbon (DOC) in water media, either by steric hindrance or binding to the specific coatings (Wang et al., 2015). Influent, post-primary wastewater and effluent are streams with high DOC: 238 mg/L, 189 mg/L and 11.5 mg/L, respectively, in which would lead to more NPs in suspension.

3.2. Calibration of spICP-MS for consecutive elemental analysis

To calibrate the spICP-MS for NPs analysis, 100 ng/L of 60 nm Au NPs and 100 ng/L of 60 nm Ag NPs were used. Signal intensity of both Au and Ag were clearly differentiated from the ionic background (Fig. 1A). The TRA employed (100 μs) was appropriate to observe the events separated from the baseline and signal corresponding to elements in solution (Fig. 1B), as reported previously (Keller et al., 2018; Montaño et al., 2014). Although the dwell time can be decreased to <100 μs to decrease the size detection limits of Ag and TiO_2 NPs (Hadioui et al., 2019), maintaining the dwell time in 100 μs has been useful to improve the signal-noise ratio when characterizing metal NPs, even at 10-fold higher solution concentration (Montaño et al., 2014). Regarding size of the reference material (60 nm Au NPs), a gaussian distribution was exhibited with a mean of 59 ± 4 nm (Fig. 1C). The calculated η_n of the reference material, as well as particle density and analyte fraction (Table S2) were used to determine the size distribution of the spiked Ag NPs. During the Ag NPs detection, the dwell time at 100 μs was useful to differentiate the events (particles) after calibration. The size distribution of 60 nm Ag NPs was also almost symmetric, with a mean size of 60 ± 3 nm. Thus, the dwell time and

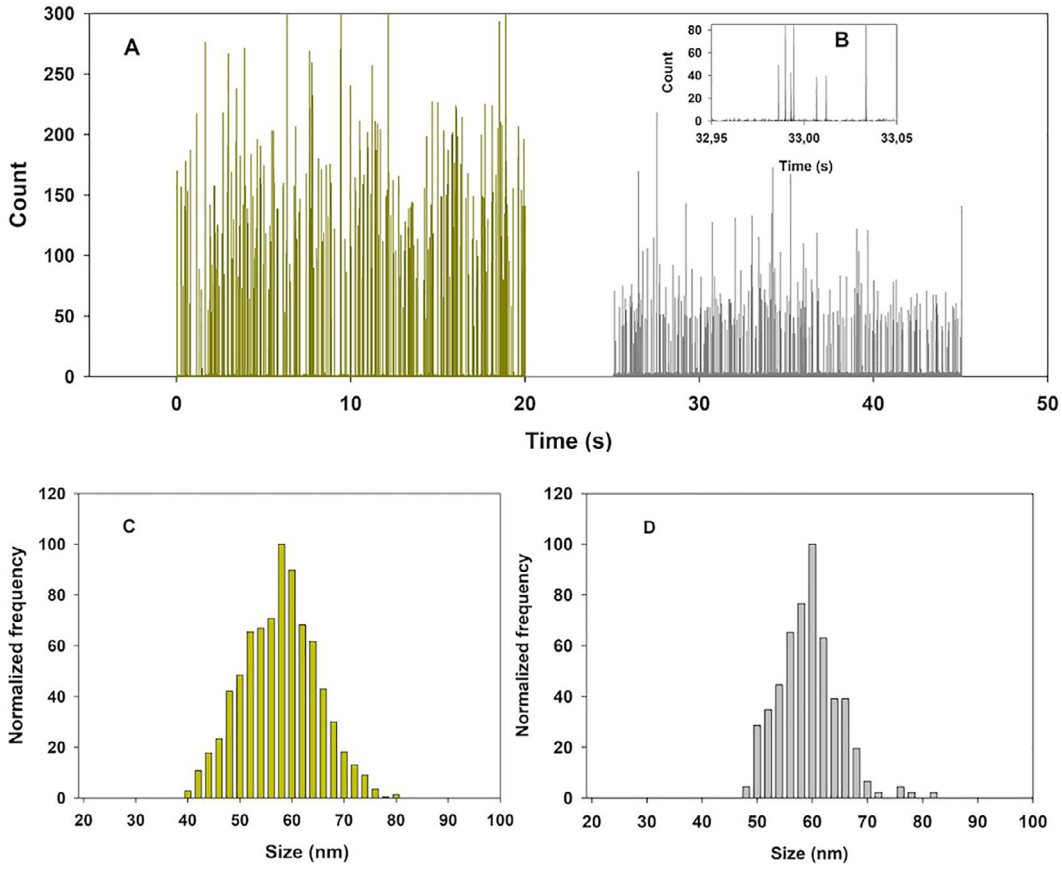

Fig. 1. Calibration of spICP-MS for elemental analysis using 60 nm Au and Ag NP reference materials. Temporal signal intensity in counts of (A) Au and (B) Ag; corresponding size distribution of (C) Au and (D) Ag NPs. .

Table 3
Concentration of Ag NPs in wastewater and sludge samples as sampled and after IER column.

Sample	Ag NPs		
	Concentration in samples (non-spiked) (ng/L)	Concentration in spike samples after IER (ng/L)	Recovery of NPs in the samples after IER (%)
Influent	11.6 ± 1.6	107.8 ± 2.1	92.9
Post-primary	10.5 ± 0.9	104.1 ± 1.8	94.2
Effluent	0.9 ± 0.2	92.3 ± 2.2	91.5
Reclaimed water	1.1 ± 0.3	88.2 ± 1.9	87.2
Waste sludge	41.5 ± 28.5	121.1 ± 4.8	85.6
Anaerobic sludge	365.2 ± 123.4	434.2 ± 2.5	93.3

calculated η_n were applied to other elements with the assumed densities and analyte mass fractions.

3.3. Metal-based nanoparticles in wastewater: difference between spICP-MS and IER-spICP-MS

The influence that the IER column have on NP adsorption was evaluated by spiking Ag NPs in the collected samples and treating them with the IER. Recovery results indicated that after spike 100 ng/L of Ag NPs, the recovery of Ag NPs ranged from 85.6% to 94.2% (Table 3). Besides, there was not a significant relation between recovery percentages and sampling sites. Some studies with Ag NPs (Azimzada et al., 2017; Hadioui et al., 2014) and ZnO NPs (Hadioui et al., 2015) found few interactions between the NP concentrations and the Chelex resin, indicating that at most 10% of the particles were removed by the Chelex resin (Hadioui et al., 2015). Pouran et al. (2013) reported that ZnO NPs can be adsorbed by Chelex carboxyl group, which in fact may occur for other metal-based NPs. Although the recoveries percentages of Ag NPs used as model NPs in our study are acceptable for non-analytical purposes, NPs based on other metal, having specific coatings or with larger size could be more sensitive to the interactions with IER. This study has the limitation of having evaluated the recovery of small-size Ag NPs. Because the recovery of larger particles could be a function of their interaction with the resin, the concentration and the size distribution of some NPs could not include larger particles retained in the resin. Therefore, it is highly recommended to carry out studies focused in the NP recovery based on their size, composition and coatings. Since the removal of NPs based on different elements in the IER may occur (Pouran et al., 2013), we based the comparison between spICP-MS and IER-spICP-MS in the removal of dissolved content basis due to ionic content is a limitation for detection of NPs.

The use of the IER before spICP-MS analysis for wastewater samples notably reduced the ionic background concentration of the 13 elements evaluated in the wastewater (Figures S3 and S4). The 13 elements in the influent, measured consecutively in a single run, were divided into three levels (A) Low concentration: Co, Cd, Au, and Ag; (B) Mid concentration: Ni, Mn, Cu, Zn and Al; and

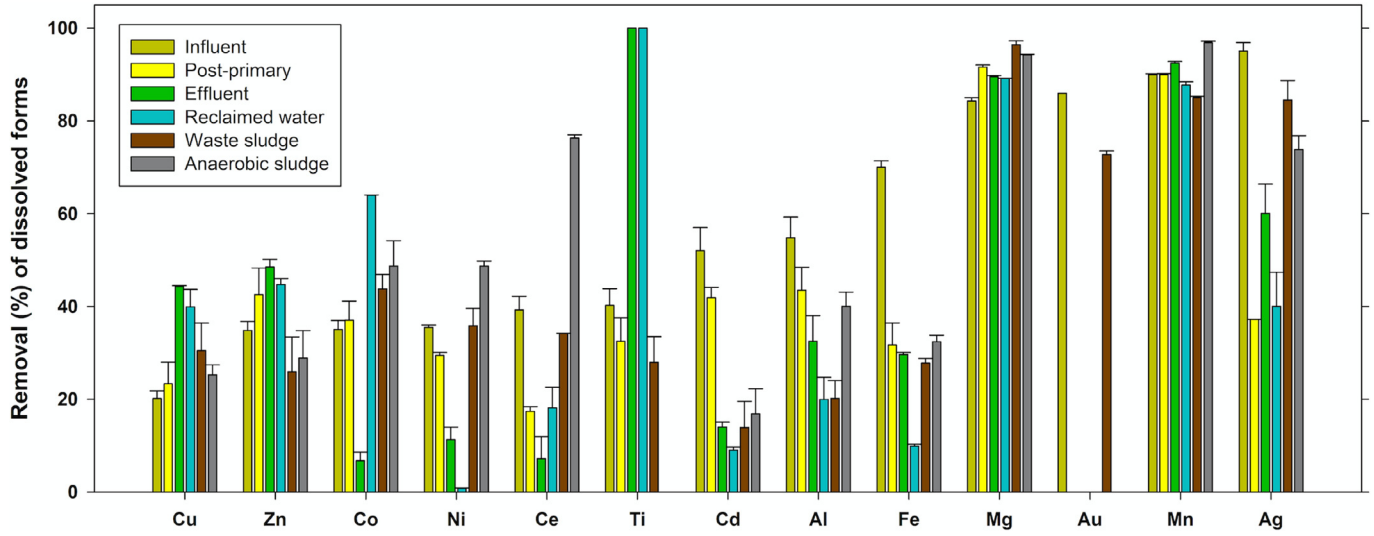

Fig. 2. Removal of the dissolved fraction of the 13 elements by the ionic exchange resin (IER) in the six matrices ($n = 3$). .

(C) High concentration: Ti, Fe, Ce and Mg (Figures S3 and S4). After IER treatment, the raw counts were reduced in the baseline. This represents the partial or full removal of the dissolved fraction of the elements, allowing better distinction of events (particles) during spICP-MS. Reducing the solubilized analytes background in wastewater, the counting of false positives was also reduced. This has been also observed for Ag NPs (Hadioui et al., 2014), even in wastewater (Azimzada et al., 2017). Our results also show that the removal of dissolved analytes was selective regarding wastewater stream and element (Fig. 2). In general, dissolved forms of the 13 elements in the influent were more removed (57%) when compared to other wastewater sources and samples of sludges. Regarding the elements, the divalent cations such as Cu^{2+}, Zn^{2+}, Mg^{2+}, Mn^{2+}, among others, had higher affinity to the IER. This is expected since the Chelex resin has presented high affinity for these cations in freshwater (Bowles et al., 2006) and seawater (Søndergaard et al., 2015), with ion removal > 80% in both cases. The differential removal also reflects the complexity of the wastewater and sludge matrices, and the fact that the concentration of dissolved analytes ions differed significantly prior to IER for the various elements, as they are removed through the treatment processes (via complexation, adsorption, precipitation, etc.).

The removal of the dissolved analytes fraction via IER influenced the size detection limit, the size distribution and the calculated mean size for the various metal-based NPs. The mean size decreased or increased depending on element, wastewater stream and whether IER was used prior to spICP-MS or not (Fig. 3). In the case of the influent, the wastewater with the highest content of analytes in solution, NPs size detection limit and size distribution were notably improved using the IER (Fig. 4). Moreover, in the influent all metal-based particles measured via IER-spICP-MS were < 300 nm, and almost all were < 100 nm (Figure S5). For example, NPs based on Al, Ag, Au, Ni, Cd and Co were < 60 nm (Fig. 4), which are smaller than those detected without the resin. This reflects the enhanced ability to detect small NPs using IER for more than one element in a single run, this is unlike when IER has been used for one element at a time (Azimzada et al., 2017). Related to the mean size of metal-based NPs in the influent, the calculated mean size decreased for 12 of 13 elements determined via IER (Fig. 3). This is in line with a previous study that measured smaller Ag NPs when using online Chelex column prior to spICP-MS (Hadioui et al., 2014). In the particular case of Mg and Mn, the high removal of ionic content (dissolved forms) of both elements by the IER in the 6 matrices (Fig. 2) allowed to detect the smaller particles that were considered as ionic background, and may explain why the mean size of NP based on these elements decreased in all matrices. Hence, this approach also is useful to measure smaller NPs of the other analyzed elements in presence of high content of organic matter and major ions.

Dissolved analytes removal results in a more accurate measurement of NP size, even in the presence of high content of organic matter (e.g. influent and sludges). The increase in the mean size of some NPs in the other wastewater streams (e.g. post-primary, effluent) cannot be neglected. Agglomeration or aggregation is the most likely explanation, since in these processes there is removal of both ionic content and organic matter. The limited changes on the mean size of NPs present in the reclaimed water also suggest the influence of organic matter and ionic strength on mean size variation, since this filtered water contains the lowest levels of organic matter and conductivity values. Thus, the change in measured mean size also depends on element and sample matrix. Although the use of IER-spICP-MS for partial removal of ionic background and the application of shorter dwell time allowed detection of smaller particles of analyzed 13 elements than reported by conventional spICP-MS (Lee et al., 2014), an improvement in the sensitivity is needed to detect the smaller particles than the current cut off point.

3.4. Incidence of NPs in the wastewater treatment process

IER-spICP-MS was applied to determine the nanoparticulate concentration for the 13 elements at various points in the wastewater treatment process. It is important to mention that the concentration and types of NPs in wastewater streams and sludge can be related to the physicochemical characteristics of the wastewater, flow of influent wastewater and to the treatment process and operating conditions (e.g. hydraulic and sludge retention times). Although equalizer tanks can dampen flow variations, variations in the content of some ions, such as chlorine and sulfur, could modify the composition of some metallic nanoparticles in the wastewater (Levard et al., 2013; Lombi et al., 2013; Sekine et al., 2015). Hence, this limitation could affect the quantification of nanoparticles in the wastewater treatment process. The measured NPs concentrations do include the natural and engineered NPs and does not include the particles that potentially were adsorbed by the IER as indicated in the previous section. Although some NPs may include

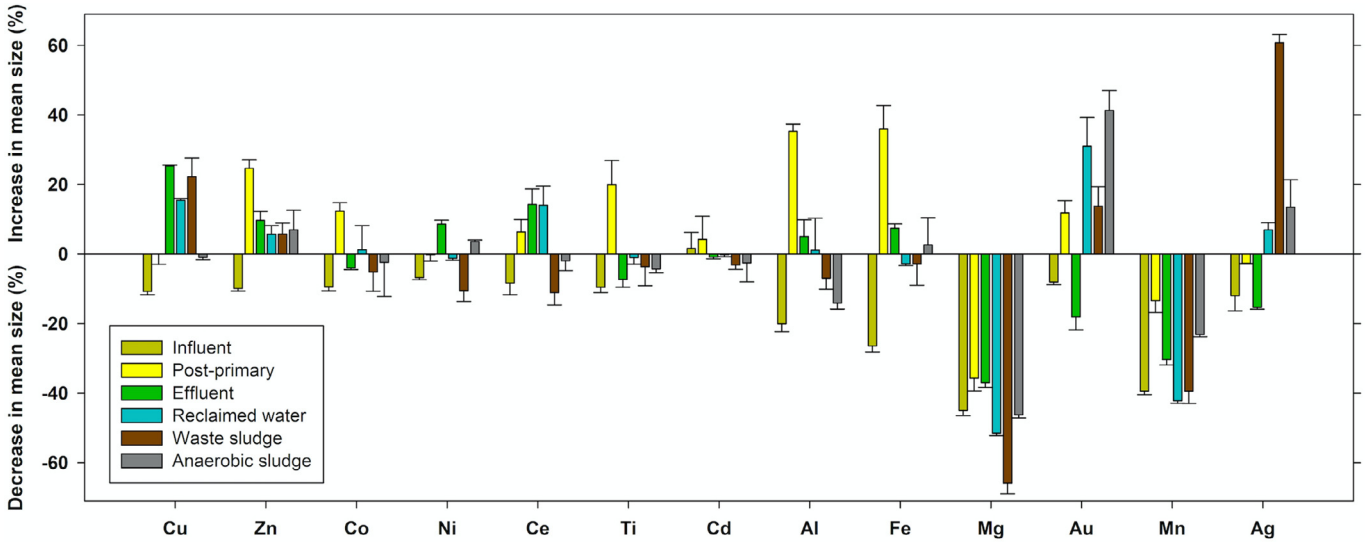

Fig. 3. Change in the calculated mean size of 13 metal-based nanoparticles in the 6 matrices, depending on whether IER was used prior to elemental analysis via spICP-MS or not. Change = [(mean size with IER – mean size without IER) / mean size without IER]•100%. Mean and relative standard deviations (RSDs), $n = 3$.

two or more elements (Bevers et al., 2020; Cervantes-Avilés et al., 2019b; Gondikas et al., 2018; Kaegi et al., 2013; Kent et al., 2014), the concentrations of NPs reported in this study assume single-element NPs since the spICP-MS measures one element at a time. Influent NP concentrations were highest (1600 to 10,700 ng/L) for elements such as Ti, Fe, Ce, Mg, Zn and Cu (Fig. 5). The concentration of Ti-based NPs was the highest (10,700 ng/L) in the influent wastewater. However, this concentration is lower than that measured in the influent of a couple of WWTPs in Norway, 154 ± 34 µg/L in LARA and 188 ± 44 µg/L in HØRA, respectively (Polesel et al., 2018), and in other studies performed in WWTP influents in Arizona, which measured mean Ti concentrations of 185–377 µg/L (Westerhoff et al., 2011). These values included the engineered and naturally occurring Ti-based nanoparticles such as Ti-silicate minerals.

The presence of aggregates based on Cu (Fig. 6), Fe, Zn, Ti and Si (Figure S6) were confirmed by transmission electron microscopy (TEM) and energy dispersive X-ray analysis (EDS) performed in a pellet of the influent sample. The high concentrations of such elements may include NPs associated with suspended solids in wastewater (Li et al., 2013), and also those NPs related to both, natural occurrence in local soils and NPs with high use in applications, likely they were released to wastewater (Keller and Lazareva, 2013). According to the concentration found after the conventional primary clarifier, this unit was able to remove a substantial fraction of most metal-based NPs, except for Fe, Mn, Ni, Cd and Al. The removal of metal-based NPs such as Ag-based in primary treatment has been also reported to range between 3% and 92% in nine WWTPs in Germany (Li et al., 2013). Hence, primary sludge (from primary treatment) can also be considered as the fate of NPs. Although there was no significance difference ($p > 0.05$) in the concentration of NPs based on Fe, Mn, Ni, Cd and Al, between influent and post-primary effluent, as the wastewater treatment train progressed, NP concentrations decreased considerably for all 13 elements. This was observed in the secondary effluent, where the maximum NP concentration was 1065 ng/L for Mg-based NPs and a minimum of 0.3 ng/L for Au-based NPs, and in reclaimed water, where only a few types of NPs exceeded 100 ng/L, namely those based on Cu (220 ng/L), Fe (274 ng/L), Ti (512 ng/L) and Mg (710 ng/L). These NPs can be considered as the major contributors to the NPs in the environment, especially to the aquatic ecosystems. Concentration of NPs based on Ag, Ti, and Zn are close to the values previously measured in wastewater influent and effluents: 100–200 ng/L of Ag (Mitrano et al., 2012), 1500–12 ng/L Ti (Li et al., 2013), and 50 ng/L of Zn (Hadioui et al., 2015). The detected concentrations of NPs in this and those studies are lower than that commonly applied in studies evaluating the ecotoxicological effects in model organisms. Therefore, future studies in organisms exposed to treated effluents could consider these low concentrations, in order to obtain a realistic scenario for organisms exposed to NPs. Moreover, these results indicate that conventional activated sludge treatment process followed by ultrafiltration systems is able to remove more than 88% of almost all evaluated the metal-based NPs, reducing the potential their effects in the environment. However, WWTP based on other technologies, such as coagulation-flocculation, trickling filters, artificial wetlands, among others, should be evaluated in terms of NPs occurrence, removal and transformation of metal-based nanoparticles. After any technology applied in the WWTP facilities, the accumulation of metal-based NPs downstream should also be evaluated as a realistic ecotoxicological scenario.

NPs in the wastewater streams within a WWTP can include zero valent metals, metal-oxides, metal-sulfides, and metal-chlorides, which are common stable forms of the metals (Kaegi et al., 2013; Lowry et al., 2012a; M. D. Montaño et al., 2014). Their formation may vary due to aerobic and anaerobic conditions in the WWTP, the concentration of major ligands, as well as the kinetics of the transformations and the residence time of the NPs in the treatment steps. These factors can be considered when performing toxicological tests in scenarios that include effluent wastewater.

Relating the measured concentrations of the metal-based NPs in this work with the predicted concentration ranges for WWTP effluent (Gottschalk et al., 2013; Hendren et al., 2013; Keller and Lazareva, 2013; Lazareva and Keller, 2014; Sun et al., 2016), several metal-NPs are within the predicted scenario. For NPs based on Ag, Ce, Ti, and Zn, the measured values are within the predicted concentration range (0.1–600 ng/L) for effluent; NPs based on Al and Fe were present in lower concentration than predicted, and Cu-based NPs were in higher concentration than predicted, reflecting higher use of Cu-based NPs than estimated or more incidental NPs based on Cu in effluent water. Since there are no predicted, or even detected, concentrations of Ni, Cd, Au, Co, Mg and Mn, this study also contributes evidence of their presence in wastewater influ-

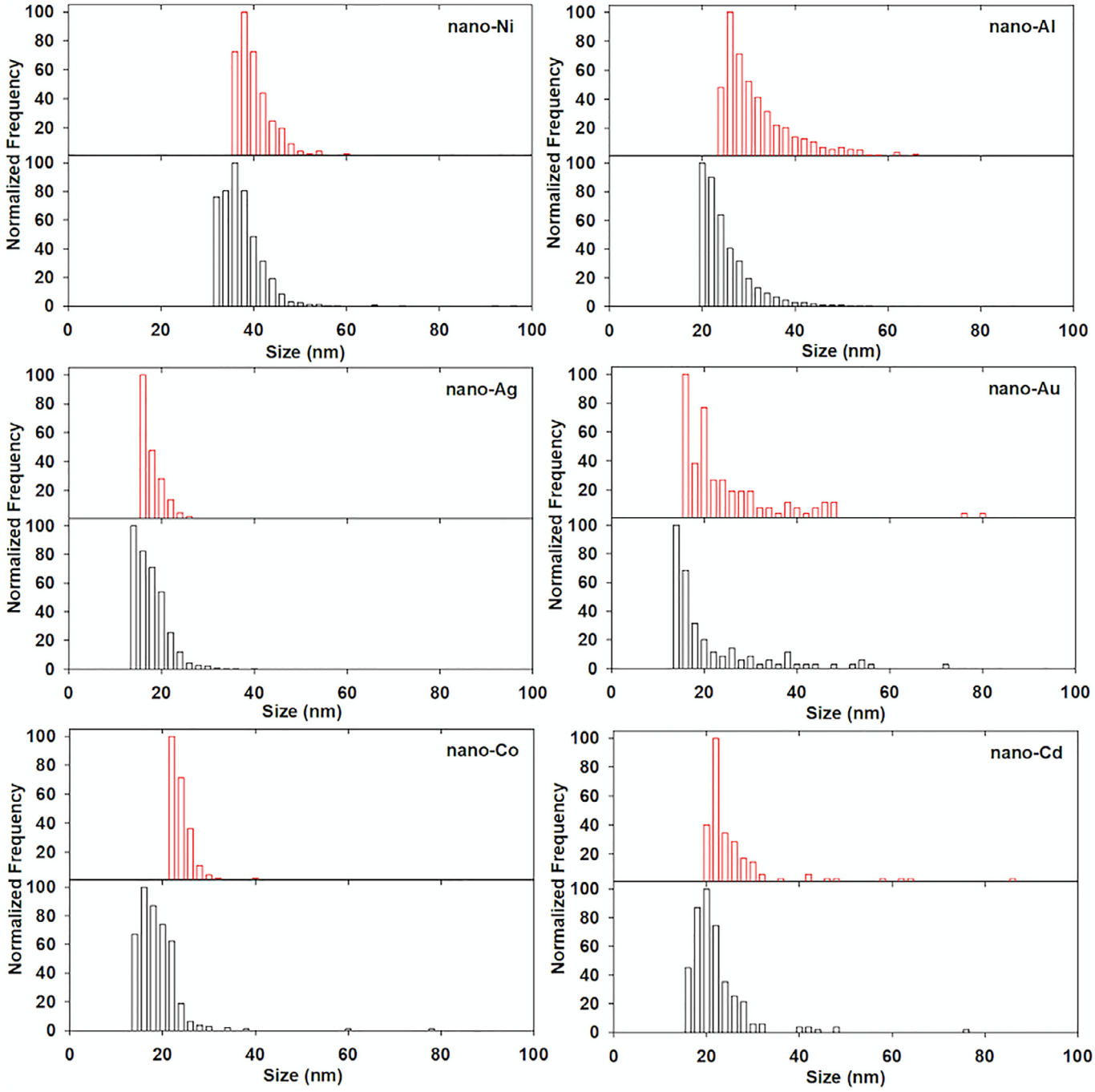

Fig. 4. Size distribution of nanoparticles based on Ni, Al, Ag, Au, Co and Cd present in the influent wastewater. Red bars correspond to the determination by conventional spICP-MS, and black bars correspond to the determination by IER-spICP-MS. To observe all elements, see supplementary information Figure S5.

ent and effluent. It should be considered that Mg compounds are added to the influent to increase the alkalinity and control the pH of the biological processes in wastewater treatment, which likely results in the formation of Mg-based NPs. Moreover, the concentration of metal-based NPs in wastewater streams will also depend on geographical location and access to treatment facilities (Keller and Lazareva, 2013; Sun et al., 2014).

Removal of NPs was observed along the wastewater treatment train. The primary clarifier removed at least 10% of the initial load of most NPs in the influent, except for Fe, Mn, Ni, Cd and Al (Fig. 7). After biological treatment (nitrification and denitrification, i.e. aerobic followed by anaerobic, then reaeration) and secondary clarifier, total load removal was more than 80% for all metal-based NPs, except for Mg and Ni. After ultra-filtration removal was 70–78% for Mg, Ni and Cd based NPs, and 88–99% for the rest of the elements considered. Given the high removal from influent to secondary effluent, the majority of metal-based NPs transfer to the sludge, as discussed below.

NPs extracted from the waste activated sludge and anaerobic sludge using centrifugation (3800 g, 10 min and 20 °C) represent around the 65% of NP present in these matrices based on previous studies (Huang et al., 2020). Moreover, the concentrations in the sludges may not reflect internalized or tightly-adsorbed NPs in the flocs (Polesel et al., 2018; Tuoriniemi et al., 2017), which must be considered in our results. Despite this and as expected, the content of metal-based NPs in the sludges was much higher than in the ef-

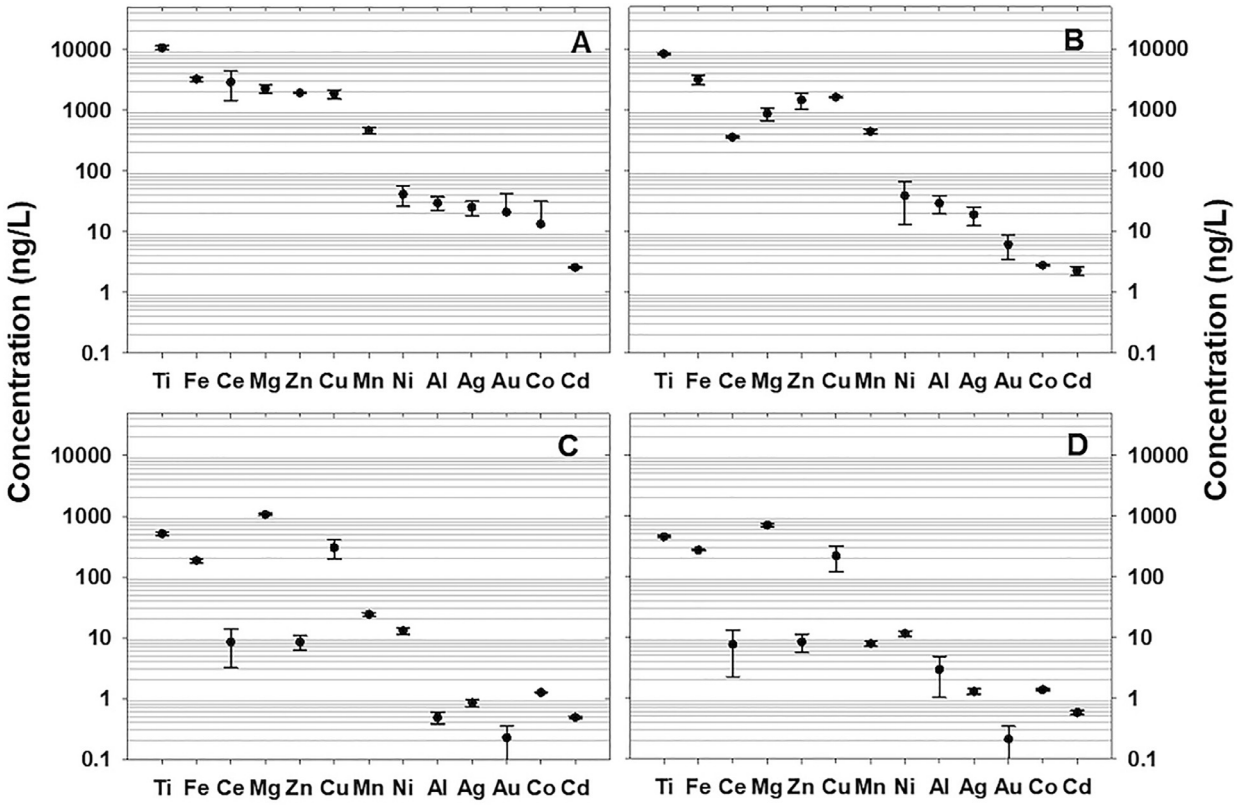

Fig. 5. Concentrations in ng/L of NPs based on 13 elements in samples collected in different points of a full-scale wastewater treatment plant. (A) Influent, (B) Post-primary, (C) Effluent and (D) Reclaimed water. Mean and relative standard deviations (RSDs), $n = 3$.

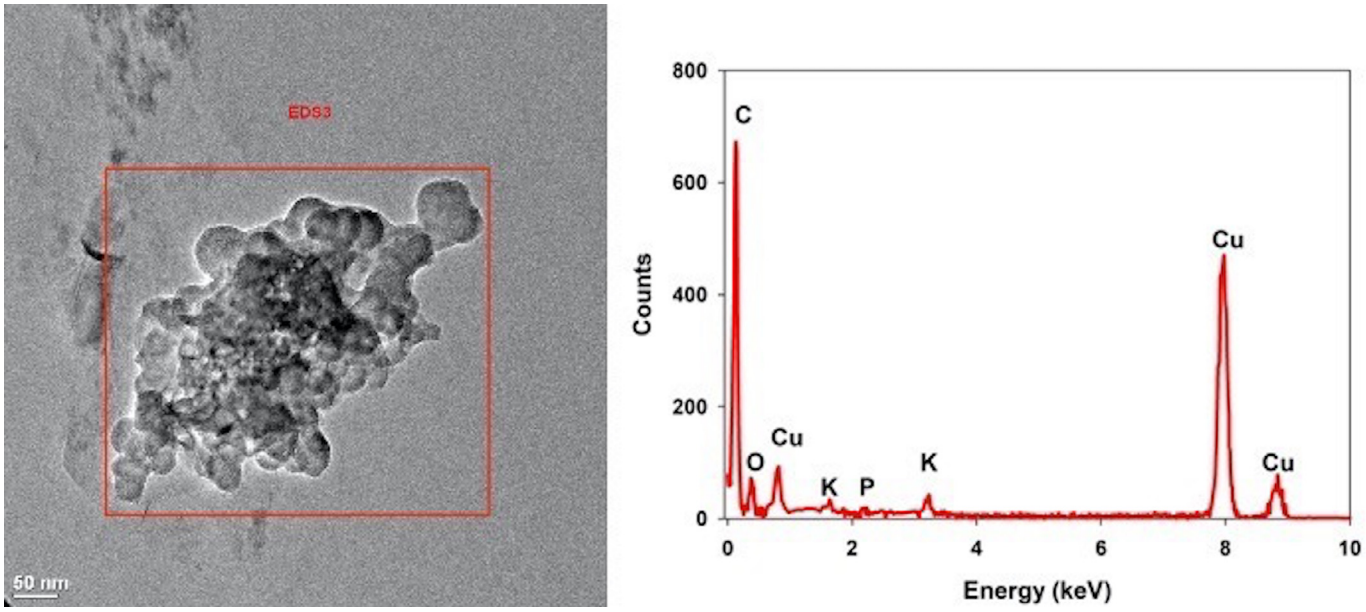

Fig. 6. Image of an aggregate of NPs based on Cu (left) acquired using transmission electron microscope (TEM), and energy dispersive X-ray (EDS) analysis (right). Nickel grids 200 mesh were used.

fluent due to their high removal in the biological processes (Fig. 8). Concentrations of metal-based NPs in the waste sludge ranged between 0.5 ng/L for Cd, up to 10,970 ng/L for Fe. The high content of Fe can be attributed to its addition for phosphorous removal during the wastewater treatment process. Hence, Fe-based NPs are expected in the waste sludge. The waste sludge is sent to the anaerobic digester where it is stored under reductive conditions for up to 10 days of hydraulic retention time. This time allows the heteroaggregation, settling, accumulation, and potential transformation of metal-based NPs due to the anaerobic conditions, such as the steady negative redox potential (−200 to −350 mV) and the high alkalinity (range of 2000 - 4000 mg $CaCO_3$/L). Based on the results in the anaerobic digester, the concentration of metal-based NPs can be divided into two groups of elements; those with low concen-

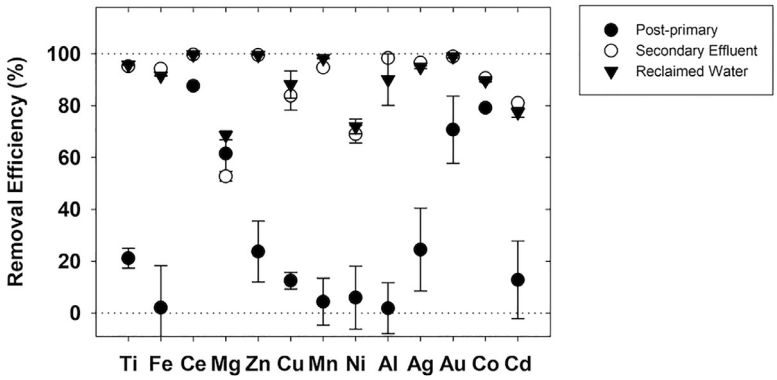

Fig. 7. Removal of metal nanoparticles based on 13 elements after different stages of wastewater treatment. Stages of the wastewater treatment include primary clarifier (post-primary), secondary clarifier (secondary effluent), and ultra-filtration membrane process (reclaimed water). Mean and relative standard deviations (RSDs), $n = 3$.

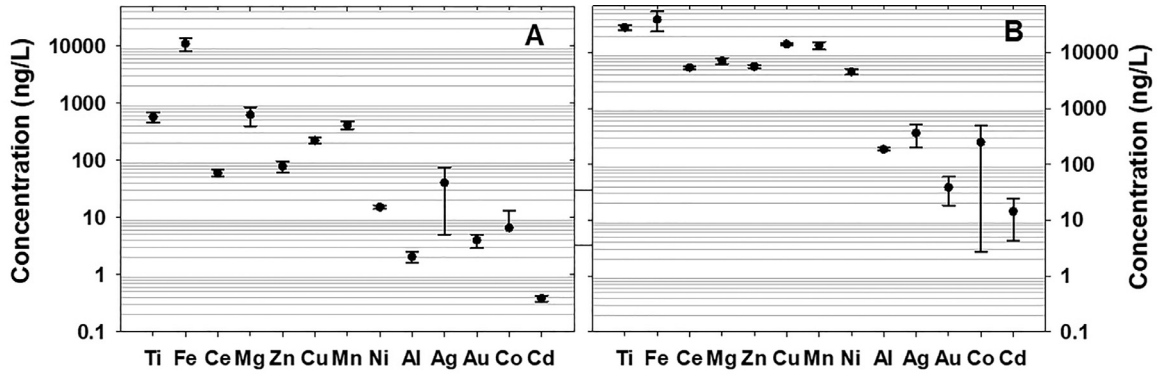

Fig. 8. Concentration of NPs based on 13 elements in samples collected in (A) waste activated sludge and in the (B) anaerobic digester. Mean and relative standard deviations (RSDs), $n = 3$.

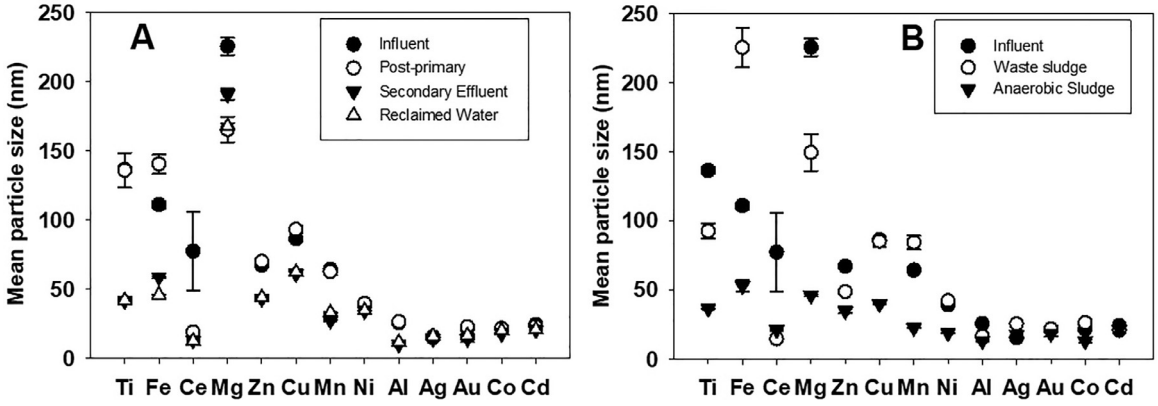

Fig. 9. Comparison of the mean size of the nanoparticles based on 13 elements detected after several steps in the (A) wastewater treatment process and in the (B) waste and anaerobic sludge.

tration (10 - 400 ng/L) such as Cd, Au, Al, Ag and Co-based NPs; and the second group with elements in high concentration (4600 – 39,900 ng/L) for Ni, Mn, Cu, Zn, Mg, Ce, Fe and Ti-based NPs. After the anaerobic digester, the main fates of these metal-based NPs are landfill and soil receiving biosolids (Lazareva and Keller, 2014). Hence, organisms in terrestrial ecosystems may be exposed to aged metal-based NPs and their transformation products via this pathway.

The mean size of the metal-based NPs in the wastewater varied as the treatment progresses (Fig. 9A). In the influent and post-primary there were no significant differences ($p > 0.05$) regarding mean size for all metal-based NPs, except for Fe, Ce and Mg (Fig. 9A). However, the mean size tended to decrease after biological treatment. In the secondary effluent and in the reclaimed water ultra-filtered by membrane with a pore size of 100 nm, the mean NP size did not change significantly ($p > 0.05$). Some solubilization and transformation is expected to occur for several of these metal-NPs during aerobic conditions (Kaegi et al., 2013), interactions with microorganisms (Tuoriniemi et al., 2017) and interaction with major ligands (Ma et al., 2013). In contrast, the NP size determined in the anaerobic sludge was smaller for almost all elements (Fig. 9B). The reducing conditions of the anaerobic digester may lead to the partial solubilization of some metal-based NPs, or their transformation to more stable forms, such as sulfides (Ma et al., 2013). Al-

though the detection and quantification of metal-based NPs of upt 13 elements was better for IER-spICP-MS than spICP-MS, the application of new analytical techniques and novel approaches to detect, quantify and differentiate from natural and engineered nanomaterials in the complex matrices is a research need to understand the real impacts on nanotechnology in aquatic ecosystems.

4. Conclusions

The incidence of NPs based on 13 different elements in different locations of a WWTP such as, influent, post-primary, effluent, reclaimed water, waste sludge and the anaerobic digester was determined via IER-spICP-MS. The IER column removed more than 50% of the dissolved fraction of the metals, which improved NP size detection limits and limited over-counting of false positives by reducing background levels. The concentration of the 13 metal-based NPs measured in the influent ranged from 2.6 ng/L for Cd-based NPs up to 10,700 ng/L for Ti-based NPs. The full-scale WWTP removed between 84 and 99% of the metal-based NPs, with the exception of Mg, Ni and Cd NPs, which were only removed 70%, 73% and 78%, respectively. The main fate of the 13 metal-based NPs was the anaerobic digester where concentrations ranged from 10 to 39,900 ng/L for the different metal-based NPs. Size discrimination of NPs was also observed along the wastewater treatment process, with smaller particles detected in the effluent (20–180 nm) than in the influent (20–300 nm) for Ti, Fe, Ce, Mg, Zn, Cu, Mn, Al, and Ni. Measured NP concentrations in WWTP effluent were generally within predicted levels, except for lower than predicted concentrations for Al and Fe, and higher than predicted for Cu-based NPs. For NP of Ni, Cd, Au, Co, Mg and Mn, this study evidence their presence in wastewater influent and effluent and can be useful for risk assessment. Although in this work the incidence of NPs determination did include natural and engineered NP, the approach done may provide valuable information regarding concentration and size distribution of NPs from 13 elements that arrives to the environment via effluent and the sludge disposal.

Declaration of Competing Interest

The authors declare that they have no known competing financial interests or personal relationships that could have appeared to influence the work reported in this paper.

Acknowledgments

Support was provided by the University of California Center for Environmental Implications of Nanotechnology, funded by the U.S. National Science Foundation and the Environmental Protection Agency under Cooperative Agreement Number DBI-0830117. Arturo A. Keller also appreciates Agilent Technologies for their Agilent Thought Leader Award. Pabel Cervantes-Aviles thanks CONACYT.

Supplementary materials

Supplementary material associated with this article can be found, in the online version, at doi:10.1016/j.watres.2020.116603.

References

APHA, 2005. Standard methods for the examination of water and wastewater. Stand. Method. 541 ISBN 9780875532356.

Azimzada, A., Tufenkji, N., Wilkinson, K.J., 2017. Transformations of silver nanoparticles in wastewater effluents: links to Ag bioavailability. Environ. Sci. Nano 4, 1339–1349. doi:10.1039/c7en00093f.

Barton, L.E., Auffan, M., Olivi, L., Bottero, J.Y., Wiesner, M.R., 2015. Heteroaggregation, transformation and fate of CeO<inf>2</inf>nanoparticles in wastewater treatment. Environ. Pollut. 203, 122–129. doi:10.1016/j.envpol.2015.03.035.

Bednar, A.J., Poda, A.R., Mitrano, D.M., Kennedy, A.J., Gray, E.P., Ranville, J.F., Hayes, C.A., Crocker, F.H., Steevens, J.A., 2013. Comparison of on-line detectors for field flow fractionation analysis of nanomaterials. Talanta 104, 140–148. doi:10.1016/j.talanta.2012.11.008.

Bevers, S., Montaño, M.D., Rybicki, L., Hofmann, T., Kammer, F.Von Der, Ranville, J.F., 2020. Quantification and Characterization of Nanoparticulate Zinc in an Urban Watershed 8, 1–16. 10.3389/fenvs.2020.00084

Bi, X., Reed, R., Westerhoff, P., 2015. Control of nanomaterials used in chemical mechanical polishing/planarization slurries during on-site industrial and municipal biological wastewater treatment. Frontiers of Nanoscience. Elsevier doi:10.1016/B978-0-08-099948-7.00008-7.

Bitragunta, S.P., Palani, S.G., Gopala, A., Sarkar, S.K., Kandukuri, V.R., 2017. Detection of TiO2 nanoparticles in municipal sewage treatment plant and their characterization using single particle ICP-MS. Bull. Environ. Contam. Toxicol. 98, 595–600. doi:10.1007/s00128-017-2031-8.

Borovinskaya, O., Hattendorf, B., Tanner, M., Gschwind, S., Günther, D., 2013. A prototype of a new inductively coupled plasma time-of-flight mass spectrometer providing temporally resolved, multi-element detection of short signals generated by single particles and droplets. J. Anal. At. Spectrom. 28, 226–233. doi:10.1039/c2ja30227f.

Bowles, K.C., Apte, S.C., Batley, G.E., Hales, L.T., Rogers, N.J., 2006. A rapid Chelex column method for the determination of metal speciation in natural waters. Anal. Chim. Acta 558, 237–245. doi:10.1016/j.aca.2005.10.071.

Cervantes-Avilés, P., Huang, Y., Keller, A.A., 2019a. Incidence and persistence of silver nanoparticles throughout the wastewater treatment process. Water Res 156, 188–198. doi:10.1016/j.watres.2019.03.031.

Cervantes-Avilés, P., Huang, Y., Keller, A.A., 2019b. Multi-technique approach to study the stability of silver nanoparticles at predicted environmental concentrations in wastewater. Water Res 166, 115072. doi:10.1016/j.watres.2019.115072.

Cervantes-Avilés, P., Ida, J., Toda, T., Cuevas-Rodríguez, G., 2018. Effects and fate of TiO2 nanoparticles in the anaerobic treatment of wastewater and waste sludge. J. Environ. Manage. 222, 227–233. doi:10.1016/j.jenvman.2018.05.074.

Choi, S., Johnston, M.V., Wang, G.S., Huang, C.P., 2017. Looking for engineered nanoparticles (ENPs) in wastewater treatment systems: qualification and quantification aspects. Sci. Total Environ. 590–591, 809–817. doi:10.1016/j.scitotenv.2017.03.061.

Contado, C., Pagnoni, A., 2010. TiO2 nano- and micro-particles in commercial foundation creams: field Flow-Fractionation techniques together with ICP-AES and SQW Voltammetry for their characterization. Anal. Method. 2, 1112–1124. doi:10.1039/c0ay00205d.

Cornelis, G., Hassellöv, M., 2014. A signal deconvolution method to discriminate smaller nanoparticles in single particle ICP-MS. J. Anal. At. Spectrom. 29, 134–144. doi:10.1039/c3ja50160d.

Degueldre, C., Favarger, P.Y., 2003. Colloid analysis by single particle inductively coupled plasma-mass spectroscopy: a feasibility study. Colloid. Surface. A Physicochem. Eng. Asp. 217, 137–142. doi:10.1016/S0927-7757(02)00568-X.

Fréchette-Viens, L., Hadioui, M., Wilkinson, K.J., 2019. Quantification of ZnO nanoparticles and other Zn containing colloids in natural waters using a high sensitivity single particle ICP-MS. Talanta 200, 156–162. doi:10.1016/j.talanta.2019.03.041.

Georgantzopoulou, A., Carvalho, P.A., Vogelsang, C., Tilahun, M., ndungu, kuria, Booth, A.M., Thomas, K.V., Macken, A.L., 2018. Ecotoxicological effects of transformed silver and titanium dioxide nanoparticles in the effluent from a lab-scale wastewater treatment system. Environ. Sci. Technol. 52. doi:10.1021/acs.est.8b01663, acs.est.8b01663.

Gondikas, A., von der Kammer, F., Kaegi, R., Borovinskaya, O., Neubauer, E., Navratilova, J., Praetorius, A., Cornelis, G., Hofmann, T., 2018. Where is the nano? Analytical approaches for the detection and quantification of TiO $_2$ engineered nanoparticles in surface waters. Environ. Sci. Nano 5, 313–326. doi:10.1039/C7EN00952F.

Gottschalk, F., Sun, T., Nowack, B., 2013. Environmental concentrations of engineered nanomaterials: review of modeling and analytical studies. Environ. Pollut. 181, 287–300. doi:10.1016/j.envpol.2013.06.003.

Guo, H., Xing, B., Hamlet, L.C., Chica, A., He, L., 2016. Surface-enhanced Raman scattering detection of silver nanoparticles in environmental and biological samples. Sci. Total Environ. 554–555, 246–252. doi:10.1016/j.scitotenv.2016.02.084.

Hadioui, M., Knapp, G., Azimzada, A., Jreije, I., Frechette-Viens, L., Wilkinson, K.J., 2019. Lowering the size detection limits of Ag and TiO2 nanoparticles by single particle ICP-MS. Anal. Chem. doi:10.1021/acs.analchem.9b04007.

Hadioui, M., Merdzan, V., Wilkinson, K.J., 2015. Detection and characterization of ZnO nanoparticles in surface and waste waters using single particle ICPMS. Environ. Sci. Technol. 49, 6141–6148. doi:10.1021/acs.est.5b00681.

Hadioui, M., Peyrot, C., Wilkinson, K.J., 2014. Improvements to single particle ICPMS by the online coupling of ion exchange resins. Anal. Chem. 86, 4668–4674. doi:10.1021/ac5004932.

Heithmar, E.M., Pergantis, S.A., 2010. Characterizing Concentrations and Size Distributions of Metal-Containing Nanoparticles in Waste Water. U.S. Environmental Protection Agency, Washington, DC.

Hendren, C.O., Badireddy, A.R., Casman, E., Wiesner, M.R., 2013. Modeling nanomaterial fate in wastewater treatment: Monte Carlo simulation of silver nanoparticles (nano-Ag). Sci. Total Environ. 449, 418–425. doi:10.1016/j.scitotenv.2013.01.078.

Hotze, E.M., Phenrat, T., Lowry, G.V., 2010. Nanoparticle aggregation: challenges to understanding transport and reactivity in the environment. J. Environ. Qual. 39, 1909. doi:10.2134/jeq2009.0462.

Huang, Y., Keller, A., Cervantes-Avilés, P., Nelson, J., 2020. Fast multi-element quantification of nanoparticles in wastewater and sludge using single particle ICP-MS. Under Rev..

Kaegi, R., Voegelin, A., Ort, C., Sinnet, B., Thalmann, B., Krismer, J., Hagendorfer, H., Elumelu, M., Mueller, E., 2013. Fate and transformation of silver nanoparticles in urban wastewater systems. Water Res 47, 3866–3877. doi:10.1016/j.watres.2012.11.060.

Kaegi, R., Voegelin, A., Sinnet, B., Zuleeg, S., Hagendorfer, H., Burkhardt, M., Siegrist, H., 2011. Behavior of metallic silver nanoparticles in a pilot wastewater treatment plant. Environ. Sci. Technol. 45, 3902–3908. doi:10.1021/es1041892.

Keller, A.A., Huang, Y., Nelson, J., 2018. Detection of nanoparticles in edible plant tissues exposed to nano-copper using single-particle ICP-MS. J. Nanoparticle Res. 20. doi:10.1007/s11051-018-4192-8.

Keller, A.A., Lazareva, A., 2013. Predicted releases of engineered nanomaterials: from global to regional to local. Environ. Sci. Technol. Lett. 1, 65–70. doi:10.1021/ez400106t.

Kent, R.D., Oser, J.G., Vikesland, P.J., 2014. Controlled evaluation of silver nanoparticle sulfidation in a full-scale wastewater treatment plant. Environ. Sci. Technol. 48, 8564–8572. doi:10.1021/es404989t.

Laborda, F., Bolea, E., Cepriá, G., Gómez, M.T., Jiménez, M.S., Pérez-Arantegui, J., Castillo, J.R., 2016. Detection, characterization and quantification of inorganic engineered nanomaterials: a review of techniques and methodological approaches for the analysis of complex samples. Anal. Chim. Acta 904, 10–32. doi:10.1016/j.aca.2015.11.008.

Laborda, F., Bolea, E., Jiménez-Lamana, J., 2014. Single particle inductively coupled plasma mass spectrometry: a powerful tool for nanoanalysis. Anal. Chem. 86, 2270–2278. doi:10.1021/ac402980q.

Laborda, F., Gimenez-Ingalaturre, A.C., Bolea, E., Castillo, J.R., 2019. Single particle inductively coupled plasma mass spectrometry as screening tool for detection of particles. Spectrochim. Acta - Part B At. Spectrosc. 159, 105654. doi:10.1016/j.sab.2019.105654.

Lazareva, A., Keller, A.A., 2014. Estimating potential life cycle releases of engineered nanomaterials from wastewater treatment plants. ACS Sustain. Chem. Eng. 2, 1656–1665. doi:10.1021/sc500121w.

Lead, J.R., Batley, G.E., Alvarez, P.J.J., Croteau, M.N., Handy, R.D., McLaughlin, M.J., Judy, J.D., Schirmer, K., 2018. Nanomaterials in the environment: behavior, fate, bioavailability, and effects—an updated review. Environ. Toxicol. Chem. 37, 2029–2063. doi:10.1002/etc.4147.

Lee, S., Bi, X., Reed, R.B., Ranville, J.F., Herckes, P., Westerhoff, P., 2014. Nanoparticle size detection limits by single particle ICP-MS for 40 elements. Environ. Sci. Technol. 48, 10291–10300. doi:10.1021/es502422v.

Levard, C., Hotze, E.M., Colman, B.P., Dale, A.L., Truong, L., Yang, X.Y., Bone, A.J., Brown, G.E., Tanguay, R.L., Di Giulio, R.T., Bernhardt, E.S., Meyer, J.N., Wiesner, M.R., Lowry, G.V., 2013. Sulfidation of silver nanoparticles: natural antidote to their toxicity. Environ. Sci. Technol. 47, 13440–13448. doi:10.1021/es403527n.

Li, L., Hartmann, G., Döblinger, M., Schuster, M., 2013. Quantification of nanoscale silver particles removal and release from municipal wastewater treatment plants in Germany. Environ. Sci. Technol. 47, 7317–7323. doi:10.1021/es3041658.

Lombi, E., Donner, E., Taheri, S., Tavakkoli, E., Jamting, Å.K., McClure, S., Naidu, R., Miller, B.W., Scheckel, K.G., Vasilev, K., 2013. Transformation of four silver/silver chloride nanoparticles during anaerobic treatment of wastewater and post-processing of sewage sludge. Env. Pollut 176, 193–197.

Lowry, G.V., Espinasse, B.P., Badireddy, A.R., Richardson, C.J., Reinsch, B.C., Bryant, L.D., Bone, A.J., Deonarine, A., Chae, S., Therezien, M., Colman, B.P., Hsu-Kim, H., Bernhardt, E.S., Matson, C.W., Wiesner, M.R., 2012a. Long-term transformation and fate of manufactured Ag nanoparticles in a simulated large scale freshwater emergent wetland. Environ. Sci. Technol. 46, 7027–7036. doi:10.1021/es204608d.

Lowry, G.V., Gregory, K.B., Apte, S.C., Lead, J.R., 2012b. Transformations of nanomaterials in the environment. Environ. Sci. Technol. 46, 400928. doi:10.1021/es300839e.

Ma, R., Levard, C., Judy, J.D., Unrine, J.M., Durenkamp, M., Martin, B., Jefferson, B., Lowry, G.V., 2013. Fate of Zinc Oxide and silver nanoparticles in a pilot wastewater treatment plant and in processed biosolids. Environ. Sci. Technol. 48, 104–112. doi:10.1021/es403646x.

Mitrano, D.M., Lesher, E.K., Bednar, A., Monserud, J., Higgins, C.P., Ranville, J.F., 2012. Detecting nanoparticulate silver using single-particle inductively coupled plasma-mass spectrometry. Environ. Toxicol. Chem. 31, 115–121. doi:10.1002/etc.719.

Montaño, M.D., Lowry, G.V., Von Der Kammer, F., Blue, J., Ranville, J.F., 2014. Current status and future direction for examining engineered nanoparticles in natural systems. Environ. Chem. 11, 351–366. doi:10.1071/EN14037.

Montaño, M.D., Von Der Kammer, F., Cuss, C.W., Ranville, J.F., 2019. Opportunities for examining the natural nanogeochemical environment using recent advances in nanoparticle analysis. J. Anal. At. Spectrom. 34, 1768–1772. doi:10.1039/c9ja00168a.

Mozhayeva, D., Engelhard, C., 2017. Separation of silver nanoparticles with different coatings by capillary electrophoresis coupled to ICP-MS in single particle mode. Anal. Chem. 89, 9767–9774. doi:10.1021/acs.analchem.7b01626.

Navratilova, J., Praetorius, A., Gondikas, A., Fabienke, W., von der Kammer, F., Hofmann, T., 2015. Detection of engineered copper nanoparticles in soil using single particle ICP-MS. Int. J. Environ. Res. Public Health 12, 15756–15768. doi:10.3390/ijerph121215020.

Ortelli, S., Badetti, E., Blosi, M., Costa, A.L., Brunelli, A., Hristozov, D., Bonetto, A., Marcomini, A., 2017. Colloidal characterization of CuO nanoparticles in biological and environmental media. Environ. Sci. Nano 4, 1264–1272. doi:10.1039/c6en00601a.

Pace, H.E., Rogers, N.J., Jarolimek, C., Coleman, V.A., Higgins, C.P., Ranville, J.F., 2011. Determining transport efficiency for the purpose of counting and sizing nanoparticles via single particle inductively coupled plasma mass spectrometry. Anal. Chem. 83, 9361–9369. doi:10.1021/ac201952t.

Palchoudhury, S., Baalousha, M., Lead, J.R., 2015. Methods for measuring concentration (mass, surface area and number) of nanomaterials. Frontiers of Nanoscience. Elsevier doi:10.1016/B978-0-08-099948-7.00005-1.

Pergantis, S.A., Jones-Lepp, T.L., Heithmar, E.M., 2012. Hydrodynamic chromatography online with single particle-inductively coupled plasma mass spectrometry for ultratrace detection of metal-containing nanoparticles. Anal. Chem. 84, 6454–6462. doi:10.1021/ac300302j.

Polesel, F., Farkas, J., Kjos, M., Almeida Carvalho, P., Flores-Alsina, X., Gernaey, K.V., Hansen, S.F., Plósz, B.G., Booth, A.M., 2018. Occurrence, characterisation and fate of (nano)particulate Ti and Ag in two Norwegian wastewater treatment plants. Water Res 141, 19–31. doi:10.1016/j.watres.2018.04.065.

Pouran, H.M., Llabjani, V., Martin, F.L., Zhang, H., 2013. Evaluation of ATR-FTIR spectroscopy with multivariate analysis to study the binding mechanisms of ZnO nanoparticles or Zn2+ to chelex-100 or metsorb. Environ. Sci. Technol. 47, 11115–11121. doi:10.1021/es4017552.

Proulx, K., Hadioui, M., Wilkinson, K.J., 2016. Separation, detection and characterization of nanomaterials in municipal wastewaters using hydrodynamic chromatography coupled to ICPMS and single particle ICPMS. Anal. Bioanal. Chem. 408, 5147–5155. doi:10.1007/s00216-016-9451-x.

Qu, H., Mudalige, T.K., Linder, S.W., 2014. Capillary electrophoresis/inductively-coupled plasma-mass spectrometry: development and optimization of a high resolution analytical tool for the size-based characterization of nanomaterials in dietary supplements. Anal. Chem. 86, 11620–11627. doi:10.1021/ac5025655.

Rathnayake, S., Unrine, J.M., Judy, J., Miller, A.F., Rao, W., Bertsch, P.M., 2014. Multitechnique investigation of the ph dependence of phosphate induced transformations of ZnO nanoparticles. Environ. Sci. Technol. 48, 4757–4764. doi:10.1021/es404544w.

Schwertfeger, D.M., Velicogna, J.R., Jesmer, A.H., Saatcioglu, S., McShane, H., Scroggins, R.P., Princz, J.I., 2017. Extracting metallic nanoparticles from soils for quantitative analysis: method development using engineered silver nanoparticles and SP-ICP-MS. Anal. Chem. 89, 2505–2513. doi:10.1021/acs.analchem.6b04668.

Sekine, R., Brunetti, G., Donner, E., Khaksar, M., Vasilev, K., Jämting, A.K., Scheckel, K.G., Kappen, P., Zhang, H., Lombi, E., 2015. Speciation and lability of Ag-, AgCl-, and Ag2S-nanoparticles in soil determined by X-ray absorption spectroscopy and diffusive gradients in thin films. Environ. Sci. Technol. 49, 897–905. doi:10.1021/es504229h.

Søndergaard, J., Asmund, G., Larsen, M.M., 2015. Trace elements determination in seawater by ICP-MS with on-line pre-concentration on a Chelex-100 column using a “standard” instrument setup. MethodsX 2, 323–330. doi:10.1016/j.mex.2015.06.003.

Sun, T.Y., Bornhöft, N.A., Hungerbühler, K., Nowack, B., 2016. Dynamic probabilistic modeling of environmental emissions of engineered nanomaterials. Environ. Sci. Technol. 50, 4701–4711. doi:10.1021/acs.est.5b05828.

Sun, T.Y., Gottschalk, F., Hungerbühler, K., Nowack, B., 2014. Comprehensive probabilistic modelling of environmental emissions of engineered nanomaterials. Environ. Pollut. 185, 69–76. doi:10.1016/j.envpol.2013.10.004.

Ta, C., Reith, F., Brugger, J., Pring, A., Lenehan, C.E., 2014. Analysis of Gold(I/III)-complexes by HPLC-ICP-MS demonstrates Gold(III) stability in surface waters. Env. Sci Technol 48, 5737–5744.

Tan, J., Liu, J., Li, M., El Hadri, H., Hackley, V.A., Zachariah, M.R., 2016. Electrospray-differential mobility hyphenated with single particle inductively coupled plasma mass spectrometry for characterization of nanoparticles and their aggregates. Anal. Chem. 88, 8548–8555. doi:10.1021/acs.analchem.6b01544.

Taurozzi, J.S., Hackley, V.A., Wiesner, M.R., 2012. Preparation of nanoparticle dispersions from powdered material using ultrasonic disruption. Spec. Publ. (NIST SP) doi:10.6028/NIST.SP.1200-2.

Tuoriniemi, J., Cornelis, G., Hassellöv, M., 2012. Size discrimination and detection capabilities of single-particle ICPMS for environmental analysis of silver nanoparticles. Anal. Chem. 84, 3965–3972. doi:10.1021/ac203005r.

Tuoriniemi, J., Jürgens, M.D., Hassellöv, M., Cornelis, G., 2017. Size dependence of silver nanoparticle removal in a wastewater treatment plant mesocosm measured by FAST single particle ICP-MS. Environ. Sci. Nano 4, 1189–1197. doi:10.1039/c6en00650g.

Wang, H., Adeleye, A.S., Huang, Y., Li, F., Keller, A.A., 2015. Heteroaggregation of nanoparticles with biocolloids and geocolloids. Adv. Colloid Interface Sci. 226, 24–36. doi:10.1016/j.cis.2015.07.002.

Wang, P., Menzies, N.W., Dennis, P.G., Guo, J., Forstner, C., Sekine, R., Lombi, E., Kappen, P., Bertsch, P.M., Kopittke, P.M., 2016. Silver nanoparticles entering soils via the wastewater-sludge-soil pathway pose low risk to plants but elevated Cl concentrations increase Ag bioavailability. Environ. Sci. Technol. 50, 8274–8281. doi:10.1021/acs.est.6b01180.

Westerhoff, P., Atkinson, A., Fortner, J., Wong, M.S., Zimmerman, J., Gardea-Torresdey, J., Ranville, J., Herckes, P., 2018. Low risk posed by engineered and incidental nanoparticles in drinking water. Nat. Nanotechnol. 13, 661–669. doi:10.1038/s41565-018-0217-9.

Westerhoff, P., Song, G., Hristovski, K., Kiser, M.A., 2011. Occurrence and removal of titanium at full scale wastewater treatment plants: implications for TiO2 nanomaterials. J. Environ. Monit. 13, 1195–1203.